Visual Servoing From 3D Straight Lines
With Central Catadioptric Cameras

Y. Mezouar[1], H. Hadj Abdelkader[1], P. Martinet[1], and F. Chaumette[2]

[1] LASMEA, 24 avenue des Landais, 63177 Aubière-France
{mezouar, hadj, martinet}@lasmea.univ-bpclermont.fr
[2] IRISA Campus de Beaulieu, Rennes-France
Francois.Chaumette@irisa.fr

Abstract. In this paper we consider the problem of controlling the six degrees of freedom of a manipulator using the projection of 3D lines in the image plane of central catadioptric systems. Most of the effort in visual servoing are devoted to points, only few works have investigated the use of lines in visual servoing with traditional cameras and none has explored the case of omnidirectional cameras. First a generic interaction matrix for the projection of 3D straight lines is derived from the projection model of the entire class of central catadioptric cameras. Then an image-based control law is designed and validated through simulation results.

1 Introduction

In the last years, the use of visual observations to control the motions of robots has been extensively studied (approach referred in the literature as visual servoing). Computer vision can provide to the robotic system a powerful way of sensing the environment and can potentially reduce or obliterate the need for environmental modeling, which is extremely important when the robotic tasks require the robot to move in unknown and/or dynamic environments.

Conventional cameras suffer from restricted field of view. Many applications in vision-based robotics, such as mobile robot localisation [6] and navigation [22], can benefit from panoramic field of view provided by omnidirectional cameras. In the literature, there have been several methods proposed for increasing the field of view of cameras systems [5]. One effective way is to combine mirrors with conventional imaging system. The obtained sensors are referred as catadioptric imaging systems. The resulting imaging systems have been termed central catadioptric when a single projection center describes the world-image mapping. From a practical view point, a single center of projection is a desirable property for an imaging system [2]. Baker and Nayar in [2] derive the entire class of catadioptric systems with a single viewpoint.

The visual servoing framework is an effective way to control robot motions from cameras observations [13]. Control of single mobile robot or formation of mobile robots appear in the literature with omnidirectional cameras in [7], [17], [21]. Visual servoing schemes are generally classified in three groups, namely

position-based, image-based and hybrid-based control [11, 13, 15]. Classical visual servoing techniques make assumptions on the link between the initial, current and desired images. They require correspondences between the visual features extracted from the initial image with those obtained from the desired one. These features are then tracked during the camera (and/or the object) motion. If these steps fail the visually based robotic task can not be achieved [8]. Typical cases of failure arise when matching joint images features is impossible (for example when no joint features belongs to initial and desired images) or when some parts of the visual features get out of the field of view during the servoing. Some methods has been proposed to resolve this deficiency based on path planning [16], switching control [9], zoom adjustment [18], geometrical and topological considerations [10], [20]. However, such strategies are sometimes delicate to adapt to generic setup.

Clearly, visual servoing applications can also benefit from cameras with a wide field of view. The interaction matrix plays a central role to design vision-based control law. It links the variations of image observations to the camera velocity. The analytical form of the interaction matrix is available for some image features (points, circles, lines, ⋯) in the case of conventional cameras [11]. As explained, omnidirectional view can be a powerfull way to overcome the problem of target visibility in visual servoing. To design an image-based visual servoing scheme, Barreto et *al.* in [4] studied the central catadioptric interaction matrix for a set of image points. This paper is mainly concerned with the use of projected lines extracted from central catadioptric images as input of a visual servoing control loop. When dealing with real environments (indoor or urban) or industrial workpiece, lines features are natural choices. Nevertheless, most of the effort in visual servoing are devoted to points [13], only few works have investigated the use of lines in visual servoing with traditional cameras (refer for example to [1], [11], [14]) and none has explored the case of omnidirectional cameras. This paper is concerned with this last issue, we derive a generic analytical form of the central catadioptric interaction matrix for lines which can be exploited to design a control law for positioning task of a six degrees of freedom manipulator.

The remainder of this paper is organized as follows. In Section 2, following the description of the central catadioptric camera model, lines projections in the image plane is studied. This is achieved using the unifying theory for central panoramic systems introduced in [12]. We present, in Section 3 a classical image-based control law we have used. In Section 4, we derive a generic analytical form of the interaction matrix for projected lines (conics) and then we focus on the case of cameras combining a parabolic mirror and an orthographic camera. In Section 5, simulated results are presented.

2 Central Catadioptric image formation of lines

In this section, we describe the projection model for central catadioptric cameras and then we focus on 3D lines features.

2.1 Camera model

As noted previously, a single center of projection is a desirable property for an imaging system. A single center implies that all lines passing through a 3D point and its projection in the image plane pass through a single point in 3D space. Conventional perspective cameras are single view point sensors. As shown in [2], a central catadioptric system can be built by combining an hyperbolic, elliptical or planar mirror with a perspective camera and a parabolic mirror with an orthographic camera. To simplify notations conventional perspective cameras will be embedded in the set of central catadioptric cameras. In [12], a unifying theory for central panoramic systems is presented. According to this generic model, all central panoramic cameras can be modeled by a central projection onto a sphere followed by a central projection onto the image plane (see Fig. 1). This generic model can be parametrized by the couple (ξ, φ) (see Tab.1 and refer to [4]).

camera	Mirror surface	ξ	φ
Parabolic	$z = \frac{x^2+y^2}{2a_p} - \frac{a_p}{2}$	1	$1 + 2p$
Hyperbolic	$\frac{(z+\frac{d}{2})^2}{a_h^2} - \frac{x^2+y^2}{b_h^2} = 1$	$\frac{d}{\sqrt{d^2+4p^2}}$	$\frac{d+2p}{\sqrt{d^2+4p^2}}$
Elliptical	$\frac{(z+\frac{d}{2})^2}{a_e^2} + \frac{x^2+y^2}{b_e^2} = 1$	$\frac{d}{\sqrt{d^2+4p^2}}$	$\frac{d-2p}{\sqrt{d^2+4p^2}}$
Planar	$z = \frac{d}{2}$	0	1
conventional	none	0	1

Table 1. Central catadioptric cameras description:
a_p, a_h, b_h, a_e, b_e depend only of the mirror intrinsic parameters d and p

Let $\mathcal{F}_c$ and $\mathcal{F}_m$ be the frames attached to the conventional camera and to the mirror respectively. In the sequel, we suppose that $\mathcal{F}_c$ and $\mathcal{F}_m$ are related by a translation along the Z-axis. The centers C and M of $\mathcal{F}_c$ and $\mathcal{F}_m$ will be termed optical center and principal projection center respectively. Let $\mathcal{X}$ be a 3D point with coordinates $\mathbf{X} = [X\ Y\ Z]^T$ with respect to $\mathcal{F}_m$. According to the generic projection model [12], $\mathcal{X}$ is projected in the image plane to a point $\mathbf{x} = [x\ y\ 1]^T$ with:

$$\mathbf{x} = \mathbf{KMf}(\mathbf{X}) \tag{1}$$

where $\mathbf{K}$ denote the triangular calibration matrix of the conventional camera, and:

$$\mathbf{M} = \begin{bmatrix} \varphi - \xi & 0 & 0 \\ 0 & \varphi - \xi & 0 \\ 0 & 0 & 1 \end{bmatrix}, \mathbf{f}(\mathbf{X}) = \begin{pmatrix} \frac{X}{Z+\xi\sqrt{X^2+Y^2+Z^2}} \\ \frac{Y}{Z+\xi\sqrt{X^2+Y^2+Z^2}} \\ 1 \end{pmatrix}$$

In the sequel, we will assume without loss of generality that the matrices $\mathbf{K}$ and $\mathbf{M}$ are equal to the identity matrix, the mapping function describing central catadioptric projection is then given by $\mathbf{x} = \mathbf{f}(\mathbf{X})$.
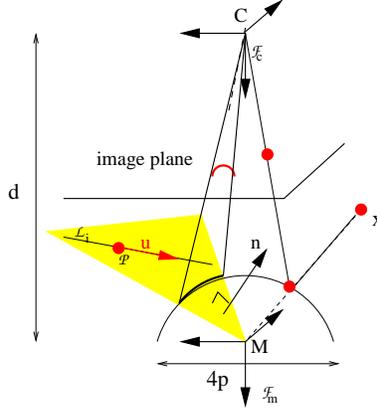
Fig. 1. Generic camera model

2.2 Projection of Lines

In order to model lines projection in the image of a central imaging system, we use the Plücker coordinates of lines (refer to Fig. 1). Let $\mathcal{P}$ be a 3D point and $\mathbf{u} = (u_x, u_y, u_z)^T$ a unit vector expressed in the mirror frame and $\mathcal{L}$ the 3-D line they define. Define $\mathbf{n} = \dfrac{\overrightarrow{M\mathcal{P}} \times \mathbf{u}}{\|\overrightarrow{M\mathcal{P}} \times \mathbf{u}\|} = (n_x, n_y, n_z)^T$ and remark that this vector is independent of the point we choose on the line. Thus the Euclidean Plücker coordinates are defined as $\mathcal{L} : \left(\mathbf{n}^T \ \mathbf{u}^T \right)^T$ with $\mathbf{n}^T \mathbf{u} = 0$. The $\mathbf{n}$-vector is orthogonal to the interpretation plane Π defined by the line and the principal projection center:

$$\mathbf{X} = [X, Y, Z]^T \in \Pi \iff n_x X + n_y Y + n_z Z = 0 \tag{2}$$

Let $\mathcal{S}$ be the intersection between the interpretation plane and the mirror surface. $\mathcal{S}$ represents the line projection in the mirror surface. The projection $\mathcal{S}$ of $\mathcal{L}$ in the image is then obtained using perspective or orthographic mapping. It can be shown (using (1), (2), and the mirror surface equations given in Tab. 1, or following [3]) that 3D points lying on $\mathcal{L}$ are mapped into points in the image $\mathbf{x}$ which verify:

$$\mathbf{x}^T \Omega \mathbf{x} = 0 \tag{3}$$

with :

$$\Omega = \begin{pmatrix} \alpha n_x^2 - n_z^\eta \xi^2 & \alpha n_x n_y & \beta n_x n_z^{\eta-1} \\ \alpha n_x n_y & \alpha n_y^2 - n_z^\eta \xi^2 & \beta n_y n_z^{\eta-1} \\ \beta n_x n_z^{\eta-1} & \beta n_y n_z^{\eta-1} & n_z^\eta \end{pmatrix}$$

where $\alpha = 1 - \xi^2$, $\beta = 2\eta - 3$, $\eta = 2$ in the general case and $\eta = 1$ for the combination parabolic mirror-orthographic camera. A line in space is thus mapped onto the image plane to a conic curve. The relation (3) defines a quadratic equation:

$$A_0 x^2 + A_1 y^2 + 2A_2 xy + 2A_3 x + 2A_4 y + A_5 = 0 \tag{4}$$

with:

$$A_0 = s\frac{n_x^2(1-\xi^2)-n_z^\eta\xi^2}{(\varphi-\xi)^2}, \quad A_1 = s\frac{n_y^2(1-\xi^2)-n_z^\eta\xi^2}{(\varphi-\xi)^2}, \quad A_2 = s\frac{n_x n_y(1-\xi^2)}{(\varphi-\xi)^2},$$
$$A_3 = s(2\eta-3)\frac{n_x n_z^{\eta-1}}{\varphi-\xi}, \quad A_4 = s(2\eta-3)\frac{n_y n_z^{\eta-1}}{\varphi-\xi}, \quad A_5 = sn_z^\eta. \tag{5}$$

Let us note that the equation (4) is defined up to a scale factor s. We thus normalize (4) using A_5 to obtain unambiguous representations, the quadratic equation is thus rewritten as follow:

$$B_0 x^2 + B_1 y^2 + 2B_2 xy + 2B_3 x + 2B_4 y + 1 = 0 \tag{6}$$

with $B_i = \frac{A_i}{A_5}$. The case $n_z = 0$ corresponds to a degenerate configuration of our representation where the optical axis lies on the interpretation plane. In the following, we consider that $n_z \neq 0$. Let us note that the normal vector $\mathbf{n}$ can be computed from (5) since $\|\mathbf{n}\| = 1$.

$$\begin{cases} n_z = (\frac{B_3^2+B_4^2}{\beta} + 1)^{-1/2} = B_n \\ n_x = \frac{B_3 B_n}{\beta} \\ n_y = \frac{B_4 B_n}{\beta} \end{cases} \tag{7}$$

Since $\mathbf{n}^T\mathbf{u} = 0$, note also that u_z can be rewritten as:

$$u_z = -\frac{B_3 u_x + B_4 u_y}{\beta} \tag{8}$$

3   Control law

Consider the vector $\mathbf{s} = (\mathbf{s_1}^T, \mathbf{s_2}^T, \cdots \mathbf{s_n}^T)^T$, where $\mathbf{s_i}$ is a m-dimensional vector containing the visual observations used as input of the image-based control scheme. If the 3D features corresponding to visual observations are motionless, the time derivative of $\mathbf{s_i}$ is:

$$\dot{\mathbf{s_i}} = \frac{\partial \mathbf{s}_i}{\partial \mathbf{r}}\frac{d\mathbf{r}}{dt} = \mathbf{J}_i\mathbf{T}$$

where $\mathbf{T}$ is a 6-dimensional vector denoting the velocity of the central catadioptric camera and containing the instantaneous angular velocity $\boldsymbol{\omega}$ and the instantaneous linear velocity $\mathbf{v}$ of a given point expressed in the mirror frame. The $m \times 6$ matrix $\mathbf{J}_i$ is the interaction matrix (or image Jacobian). It links the variation of the visual observations to the camera velocity. If we consider the time derivative of $\mathbf{s}$, the corresponding interaction matrix is $\mathbf{J} = (\mathbf{J}_i, \cdots, \mathbf{J}_n)^T$ and $\dot{\mathbf{s}} = \mathbf{J}\mathbf{T}$. To design an image-based control law, we use the task function approach introduced by Samson et *al* in [19]. Consider the following task function $\mathbf{e}$ to be regulated to $\mathbf{0}$:

$$\mathbf{e} = \widehat{\mathbf{J}}^+(\mathbf{s} - \mathbf{s}^*)$$

where $\mathbf{s}^*$ is the desired value of the observation vector $\mathbf{s}$ and $\widehat{\mathbf{J}}^+$ is the pseudo-inverse of a chosen model of $\mathbf{J}$. The time derivative of the task function is:

$$\dot{\mathbf{e}} = \frac{d\widehat{\mathbf{J}}^+}{dt}(\mathbf{s} - \mathbf{s}^*) + \widehat{\mathbf{J}}^+\dot{\mathbf{s}} = (\mathbf{O}(\mathbf{s} - \mathbf{s}^*) + \widehat{\mathbf{J}}^+\mathbf{J})\mathbf{T}$$

$\mathbf{O}(\mathbf{s} - \mathbf{s}^*)$ is a 6-dimensional square matrix such that $(\mathbf{O}(\mathbf{s} - \mathbf{s}^*)|_{\mathbf{s}=\mathbf{s}^*} = \mathbf{0}$ If we consider the following control law:

$$\mathbf{T} = -\lambda\mathbf{e} = -\lambda\widehat{\mathbf{J}}^+(\mathbf{s} - \mathbf{s}^*) \tag{9}$$

then the closed-loop system is $\dot{\mathbf{e}} = -\lambda(\mathbf{O}(\mathbf{s} - \mathbf{s}^*) + \widehat{\mathbf{J}}^+\mathbf{J})\mathbf{e}$. It is well know that such system is locally asymptotically stable in a neighbourhood of $\mathbf{s}^*$ if and only if $\widehat{\mathbf{J}}^+\mathbf{J}$ is a positive defined matrix. In order to compute the control law (9) it is necessary to provide an approximated interaction matrix $\widehat{\mathbf{J}}$. In the sequel, we derive from the projection model of line for central catadioptric cameras a generic analytical form of the interaction matrix.

4   Interaction matrix for conics

In this section, first we study a generic formulation for the image Jacobian of projected lines (conics) and then we derive from this generic formulation the image Jacobian for paracatadioptric cameras.

4.1   Generic Image Jacobian

Let us first define the observation vector $\mathbf{s}_i$ for a projected line (conic) in the central catadioptric image as:

$$\mathbf{s}_i = \begin{bmatrix} B_0 \ B_1 \ B_2 \ B_3 \ B_4 \end{bmatrix}^T \tag{10}$$

and the observation vector for n conics as $\mathbf{s} = (\mathbf{s}_1^T \cdots \mathbf{s}_n^T)^T$. Note that the observation vector is minimal for a general conic and represents without ambiguities a generic planar conic since such curves are defined by 5 parameters and defined without ambiguities by equation (6). As we will see in the sequel, the observation vector can be reduced for particular central catadioptric cameras such as the parabolic one. The interaction matrix for the observation vector $\mathbf{s}_n$ is:

$$\mathbf{J}_i = \frac{\partial \mathbf{s}_i}{\partial \mathbf{r}} = \frac{\partial \mathbf{s}_i}{\partial \mathbf{n}_i}\frac{\partial \mathbf{n}_i}{\partial \mathbf{r}} = \mathbf{J}_{sni}\mathbf{J}_{ni} \tag{11}$$

where $\mathbf{n}_i = (n_{xi}, n_{yi}, n_{zi})^T$ is the normal vector to the interpretation plane for line $\mathcal{L}_i$ expressed in the mirror frame, $\mathbf{J}_{sni}$ represents the interaction between the visual observation motion and the normal vector variation, and $\mathbf{J}_{ni}$ links the normal variations to the camera motions. It can easily be shown that [1]:

$$\begin{cases} \dot{\mathbf{u}}_i = -\boldsymbol{\omega} \times \mathbf{u}_i \\ \\ \dot{\mathbf{n}}_i = \frac{\partial \mathbf{n}_i}{\partial \mathbf{r}}\mathbf{T} = -\mathbf{v} \times \mathbf{u} - \boldsymbol{\omega} \times \mathbf{n}_i \end{cases}$$

According to the previous equations (7) and (8), the interaction between the normal vector and the camera motion is thus:

$$
\mathbf{J}_{ni} = \begin{pmatrix} 0 & \frac{B_3 u_x + B_4 u_y}{\beta} & u_y & 0 & -B_n & \frac{B_4 B_n}{\beta} \\ -\frac{B_3 u_x + B_4 u_y}{\beta} & 0 & -u_x & B_n & 0 & -\frac{B_3 B_n}{\beta} \\ -u_y & u_x & 0 & -\frac{B_4 B_n}{\beta} & \frac{B_3 B_n}{\beta} & 0 \end{pmatrix} \tag{12}
$$

The Jacobian $\mathbf{J}_{sni}$ is obtained by computing the partial derivative of (10) with respect to $\mathbf{n}_i$ and according to (7):

$$
\mathbf{J}_{sni} = \frac{1}{\beta B_n^\eta} \begin{pmatrix} 2\alpha B_3 B_n & 0 & -\frac{\eta\alpha}{\beta} B_3^2 B_n \\ 0 & 2\alpha B_4 B_n & -\frac{\eta\alpha}{\beta} B_4^2 B_n \\ \alpha B_4 B_n & \alpha B_3 B_n & -\frac{\eta\alpha}{\beta} B_3 B_4 B_n \\ \beta^2 B_n^{\eta-1} & 0 & -\beta B_3 B_n^{\eta-1} \\ 0 & \beta^2 B_n^{\eta-1} & -\beta B_4 B_n^{\eta-1} \end{pmatrix} \tag{13}
$$

The interaction matrix can finally be computed by combining the equations (12) and (13) according to relation (11). Note that the rank of the interaction matrix given by (11) is 2. At least three lines are thus necessary to control the 6 *dof* of a robotic arm. As previously explained, a chosen estimation of the interaction matrix is used to design the control law. The value of $\mathbf{J}$ at the desired position is a typical choice. In this case, the 3D parameters have to be estimated only for the desired position. In the next part, we study the particular case of paracatadioptric camera (parabolic mirror combined to orthographic camera).

4.2 A case study: paracatadioptric cameras

In the case of paracatadioptric cameras, we have $\xi = 1$, $\alpha = 0$ and $\eta = 1$. The lines are projected onto the image plane as circles or ellipses if the pixels are not square. It can be noticed that $A_2 = 0$ and $A_0 = A_1 = -A_5$ and thus the observation vector can be reduced as $\mathbf{s_i} = [B_3\ B_4]^T$. Note also that if the pixels are square a line is projected as circle of center $x = B_3$, $y = B_4$ and radius $B_3^2 + B_4^2 - 1$. Minimizing the task function $\mathbf{e}$ can thus be interpreted as minimizing the distance between current and desired centers of circles by moving the camera. According to equation (13), the Jacobian $\mathbf{J}_{sni}$ can be reduced as follow:

$$
\mathbf{J}_{sni} = \frac{1}{B_n} \begin{pmatrix} \beta & 0 & -B_3 \\ 0 & \beta & -B_4 \end{pmatrix}
$$

and by combining the previous relation with equation (12), the image Jacobian can be written:

$$
\mathbf{J} = \frac{1}{B_n} \begin{pmatrix} -u_y B_3 & -u_y B_4 & -u_y \beta & -\frac{B_3 B_4 B_n}{\beta} & \beta B_n + \frac{B_3^2 B_n}{\beta} & -B_4 B_n \\ u_x B_3 & u_x B_4 & u_x \beta & -\beta B_n - \frac{B_4^2 B_n}{\beta} & \frac{B_3 B_4 B_n}{\beta} & B_3 B_n \end{pmatrix}
$$

The rank of the image Jacobian is 2. Its kernel is spanned by the basis composed of the vectors:

$$\begin{cases} (0,\ 1,\ \frac{B_4}{\beta},\ 0,\ 0,\ 0) \\[2mm] (0,\ 0,\ -\frac{B_4 B_n (B_3^2 + B^2 + B_4^2)}{\beta^2 (u_y B_3 - u_x B_4)},\ 1,\ 0,\ \frac{(u_y B^3 + u_y B_4^2 \beta + u_x B_3^2 B_4 u_y - u_x^2 B_3 B_4^2)}{\beta}) \\[2mm] (1,\ 0,\ -\frac{B_3}{\beta},\ 0,\ 0,\ 0) \\[2mm] (0,\ 0,\ \frac{B_3 B_n (\beta^4 + B_3^2 \beta^2 + B_4^2 u_y B_3 - B_4^3 u_x)}{\beta^2},\ 0,\ 1,\ -\frac{u_x B_3^2 + u_y B_3 B_4 + u_x B^2}{\beta (u_y B_3 - u_x B_4)}) \end{cases}$$

The six degrees of freedom of a robotic arm can thus be fully controlled using three projected lines as long as the lines define three different interpretations planes.

5 Simulation results

In this section, we present simulation results of central catadioptric visual servoing from lines by using the control law (9). The value of $\mathbf{J}$ at the desired position has been used. We have considered two positioning tasks. From an initial position, the robot has to reach a desired position expressed as a desired observation vector. The first simulation concerns a camera combining an hyperbolic mirror and a perspective camera (Fig. 3). The second simulation concerns a camera combining a parabolic mirror and an orthographic camera (Fig. 4). The initial attitude of the camera with respect to the world frame is given by $\mathbf{r}_i = [0,\ 0,\ 1,\ 0,\ 0,\ 0]^T$ (the first three components are the translations in meter and the last three are the rotations in radian). The desired image corresponds to the camera configuration given by $\mathbf{r}_d = [0.1,\ 0.1,\ 1.1,\ \frac{\pi}{8},\ \frac{\pi}{8},\ \frac{\pi}{8}]^T$ in the world frame. The three lines are defined in the world space by the following Plücker coordinates:

$$\mathcal{L}_1 : \begin{pmatrix} u_1 = (0\ 1\ 0)^T \\ n_1 = (0\ 0\ -1)^T \end{pmatrix} \qquad \mathcal{L}_2 : \begin{pmatrix} u_2 = (0\ 0.9806\ 0.1961)^T \\ n_2 = (0\ -0.1961\ 0.9806)^T \end{pmatrix}$$

$$\mathcal{L}_3 : \begin{pmatrix} u_3 = (0.9623\ 0.1925\ 0.1925)^T \\ n_3 = (0.1961\ 0\ -0.9806)^T \end{pmatrix}$$

Figure 2 shows the initial spatial configurations of lines and camera. Image noise has been introduced (additive noise with maximum amplitude of 1 pixel) in the observation vectors. The Plücker coordinates of the considered lines with respect to the world frame have been corrupted with errors of maximal amplitude of 5% (these errors corrupt the estimation of the interaction matrix at the desired configuration). The images corresponding to the initial and desired cameras positions are given in Figures 3(a) and 3(b) for the hyperbolic-perspective camera 4(a) and 4(b) for the parabolic-orthographic camera. Figures 3(c) and 4(c) shows the trajectories of the conics in the image plane. Camera velocities are given in Figures 3(g), 3(h) and 4(g), 4(h). As can been seen in Figures showing the errors between desired and current observation vectors (Figs. 3(d), 3(e), 3(f) and 4(d),

4(e), 3(f)), the positioning task is correctly realized as well for the hyperbolic-perspective camera as for the parabolic-orthographic camera. Note finally, that these results confirm that visual servoing schemes can benefit from the use of central catadioptric vision systems to cope with visibility constraints.

6   Conclusions

Visibility constraints are extremely important for visual servoing applications. To overcome these constraints, the wide field of view of central catadioptric cameras can be exploited. We have addressed the problem of controlling a robotic arm by incorporating observations from a central catadioptric camera. A generic image Jacobian has been derived from the model of line projection and a control law designed. The proposed approach will be used to control a six degrees of freedom manipulator. Future work will be devoted to study the case of nonholonomic robots and path planning in central catadioptric image space.

Acknowledgment

References

1. N. Andreff, B. Espiau, and R. Horaud. Visual servoing from lines. *International Journal of Robotics Research*, 21(8):679–700, August 2002.
2. S. Baker and S. K. Nayar. A theory of single-viewpoint catadioptric image formation. *International Journal of Computer Vision*, 35(2):1–22, November 1999.
3. J. Barreto and H. Araujo. Geometric properties of central catadioptric line images. In *7th European Conference on Computer Vision, ECCV'02*, pages 237–251, Copenhagen, Denmark, May 2002.
4. J. P. Barreto, F. Martin, and R. Horaud. Visual servoing/tracking using central catadioptric images. In *ISER2002 - 8th International Symposium on Experimental Robotics*, pages 863–869, Bombay, India, July 2002.
5. R. Benosman and S. Kang. *Panoramic Vision*. Springer Verlag, 2000.
6. P. Blaer and P.K. Allen. Topological mobile robot localization using fast vision techniques. In *IEEE International Conference on Robotics and Automation*, pages 1031–1036, Washington, USA, May 2002.
7. D. Burshka, J. Geiman, and G. Hager. Optimal landmark configuration for vision based control of mobile robot. In *IEEE International Conference on Robotics and Automation*, pages 3917–3922, Tapei, Taiwan, September 2003.
8. F. Chaumette. Potential problems of stability and convergence in image-based and position-based visual servoing. *The Confluence of Vision and Control, D. Kriegman, G. Hager, A. Morse (eds), LNCIS Series, Springer Verlag*, 237:66–78, 1998.
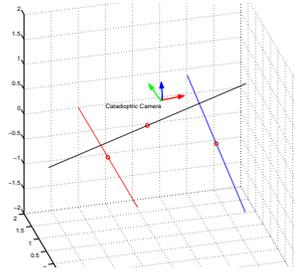
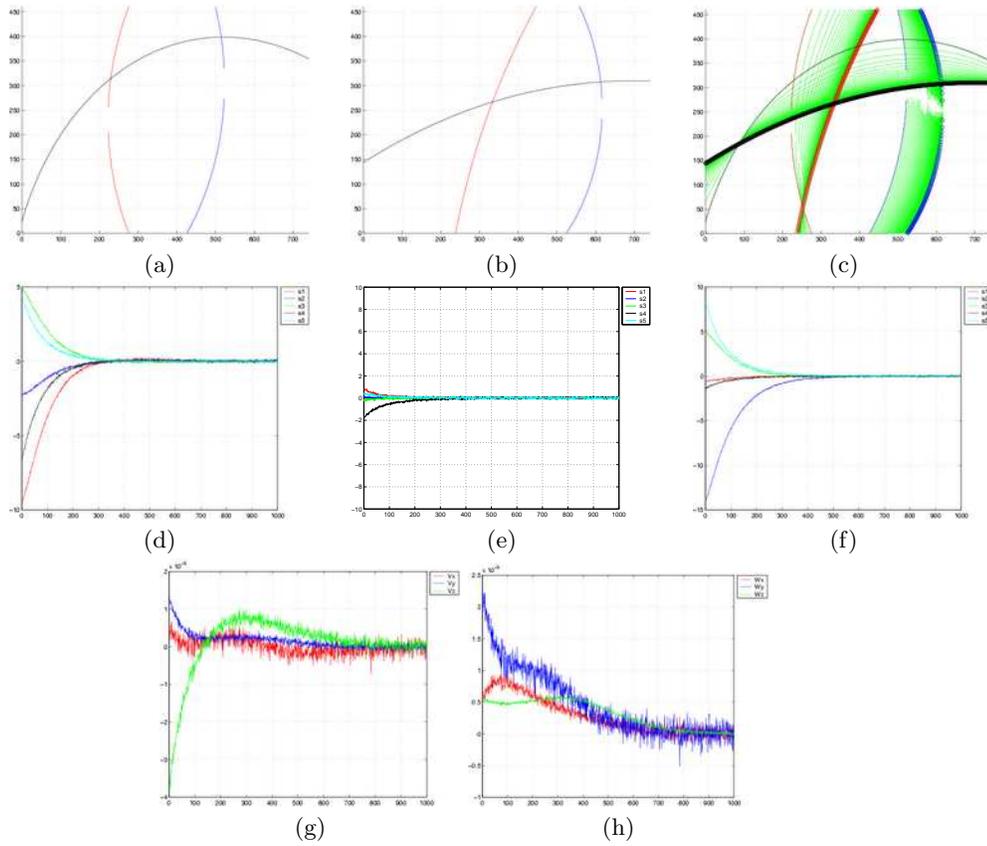**Fig. 2.** Lines configurations in 3D

Fig. 3. Hyperbolic mirror-perspective camera: (a) Initial image, (b) desired image, (c) trajectories in the image plane of line projection; Errors $(\mathbf{s}-\mathbf{s}^*)$: (d) Errors for the first conic, (e) Errors for the second conic, (f) Errors for the third conic; (g) Translational velocities [m/s] and (h) rotational velocities [rad/s]
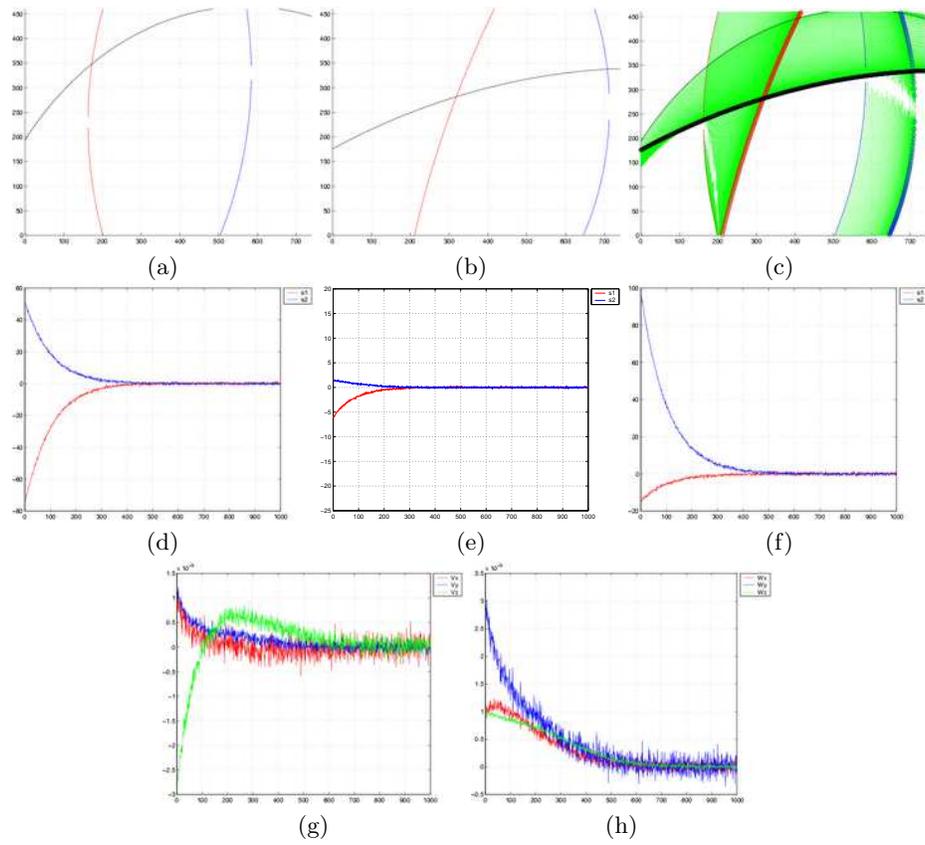
Fig. 4. Parabolic mirror-orthographic camera: (a) Initial image , (b) desired image (c) trajectory of the catadioptric image lines; Errors $(\mathbf{s} - \mathbf{s}^*)$: (d) Errors for the first conic, (e) Errors for the second conic, (f) Errors for the third conic;(g) Translational velocities [m/s] and (h) rotational velocities [rad/s]

9. G. Chesi, K. Hashimoto, D. Prattichizzo, and A. Vicino. A switching control law for keeping features in the field of view in eye-in-hand visual servoing. In *IEEE International Conference on Robotics and Automation*, pages 3929–3934, Taipei, Taiwan, September 2003.

10. Noah J. Cowan, Joel D. Weingarten, and Daniel E. Koditschek. Visual servoing via navigation functions. *IEEE Transactions on Robotics and Automation*, 18(4):521–533, August 2002.

11. B. Espiau, F. Chaumette, and P. Rives. A new approach to visual servoing in robotics. *IEEE Transactions on Robotics and Automation*, 8(3):313–326, June 1992.

12. C. Geyer and K. Daniilidis. A unifying theory for central panoramic systems and practical implications. In *European Conference on Computer Vision*, volume 29, pages 159–179, Dublin, Ireland, May 2000.

13. S. Hutchinson, G.D. Hager, and P.I. Corke. A tutorial on visual servo control. *IEEE Transactions on Robotics and Automation*, 12(5):651–670, October 1996.

14. E. Malis, J. Borrelly, and P. Rives. Intrinsics-free visual servoing with respect to straight lines. In *IEEE/RSJ International Conference on Intelligent Robots Systems*, Lausanne, Switzerland, October 2002.

15. E. Malis, F. Chaumette, and S. Boudet. 2 1/2 d visual servoing. *IEEE Transactions on Robotics and Automation*, 15(2):238–250, April 1999.

16. Y. Mezouar and F. Chaumette. Path planning for robust image-based control. *IEEE Transactions on Robotics and Automation*, 18(4):534–549, August 2002.

17. A. Paulino and H. Araujo. Multiple robots in geometric formation: Control structure and sensing. In *International Symposium on Intelligent Robotic Systems*, pages 103–112, University of Reading, UK, July 2000.

18. E. Malis S. Benhimane. Vision-based control with respect to planar and non-planar objects using a zooming camera. In *IEEE International Conference on Advanced Robotics*, pages 863–869, July 2003.

19. C. Samson, B. Espiau, and M. Le Borgne. *Robot Control : The Task Function Approach*. Oxford University Press, 1991.

20. B. Thuilot, P. Martinet, L. Cordesses, and J. Gallice. Position-based visual servoing: keeping the object in the field of vision. In *IEEE International Conference on Robotics and Automation*, pages 1624–1629, Washington DC, USA, May 2002.

21. R. Vidal, O. Shakernia, and S. Sastry. Formation control of nonholonomic mobile robots with omnidirectional visual servoing and motion segmentation. In *IEEE International Conference on Robotics and Automation*, Taipei, Taiwan, September 2003.

22. N. Winter, J. Gaspar, G. Lacey, and J. Santos-Victor. Omnidirectional vision for robot navigation. In *Proc. IEEE Workshop on Omnidirectional Vision, OMNIVIS*, pages 21–28, South Carolina, USA, June 2000.